Ninth International Conference on
THIN-WALLED STRUCTURES – ICTWS2023
Sydney, Australia, Nov 29 – Dec 1, 2023

ON THE EFFECT OF PREBUCKLING DEFLECTIONS ON THE LATERAL-TORSIONAL BUCKLING OF BEAMS

Ghaith A. Abu Reden*and Sandor Adany*[×]

* Budapest University of Technology and Economics
e-mails: ghaith.abureden@emk.bme.hu, adany.sandor@emk.bme.hu

[×] Johns Hopkins University
e-mail: asandor2@jhu.edu

Keywords: Lateral-Torsional Buckling; Prebuckling deflection; Analytical solution; Finite Element Analysis.

Abstract. *In this research the effect of prebuckling in-plane deflections on the critical moment to lateral-torsional buckling of beams is investigated. Though this topic is already discussed in the literature, the relevant papers show that there are some discrepancies in the proposals and results from the various authors. In this paper numerical studies are reported, conducted primarily by beam and shell finite element calculations. The critical moment values were calculated with and without considering the effect of prebuckling deflection. The results partly justify the conclusions from previous papers, but they also show that the effect of prebuckling deflection is greatly influenced by several parameters, such as the supports or the cross-sections shape. Unlike suggested by previous research, our results show that the prebuckling effect can be negative. In general, the results highlight that our understanding of the prebuckling deflection on the critical moment is insufficient, therefore further analytical and numerical studies are necessary.*

1 INTRODUCTION

Lateral-torsional buckling (LTB) is a classic type of instability of beams. A traditional way to stability problems is to assume a perfectly elastic and imperfection-free structure, but to consider the quadratic (i.e., nonlinear) terms in the geometric equations, which approach is called linear buckling analysis (LBA). LBA leads to critical load factors and buckled shapes. Though stability phenomena are influenced by the imperfections, still, LBA is involved in many design procedures, including those for LTB, where the critical moment is employed.

In classic LBA, the equations to be solved (either differential equations or energy equations) are written on the original, undeformed structure. It was observed, however, that the primary, first-order deformations might influence the solution. As the load is increased on the structure, the primary deflections increase, and by the time when buckling occurs, the structure is already deflected. If this deflected shape (which is independent of the imperfections, since it exists even if the original structure is perfect) is considered in the LBA, the associated critical load is different from the one without considering the prebuckling deflection. Whether the effect of the prebuckling deflection is important or not, is dependent on the structure.

In the case of beams subjected to LTB, the effect of the prebuckling deflection was included even in the very first analytical solution for the LTB problem, in 1899, by Michell [1], though his solution is valid only for beams with negligible warping. Later, it is mostly the solution without the prebuckling deflection effect became widely known, from the work of Timoshenko, who clarified the importance of warping, and published the well-known classic formula for the critical moment for LTB [2]. The influence of prebuckling displacement is discussed in a relatively small number of papers, e.g., in [3-8]. In most of these papers some analytical formula is proposed.

There seems to be a consensus in the available literature that the prebuckling deformations increase the critical moment, and that the increment is dominantly determined by the lateral rigidity of the beam. However, there are some discrepancies, too, both in the proposed analytical expressions and in the numerical results. Moreover, the reported researches mostly focused on the simplest case of LTB, namely: simply supported single-span beams, subjected to uniform bending, and with doubly symmetric I-shaped cross-sections. Other cases are hardly investigated.

In this paper the effect of prebuckling deflection on the critical moment is investigated by conducting numerical parametric studies. The main goal of these studies was to identify those factors that (might) have important influence on the effect of prebuckling deflection. Accordingly, in the completed calculations various beam lengths, various cross-section shapes, various end supports, and various loading situations have been considered. The results of the available analytical solutions are compared to those from beam finite element and shell finite element analyses. Though the completed studies are far from being comprehensive, the results show that the phenomenon is not well understood yet, as will be clear from the paper.

2 NUMERICAL STUDIES: BASIC CASE

2.1 General

In this Section the basic case is presented and discussed, "basic case" meaning that the beam is a single-span beam, with forked supports, subjected to uniform bending, and the beam has doubly symmetric cross-section. It is illustrated in Fig. 1.

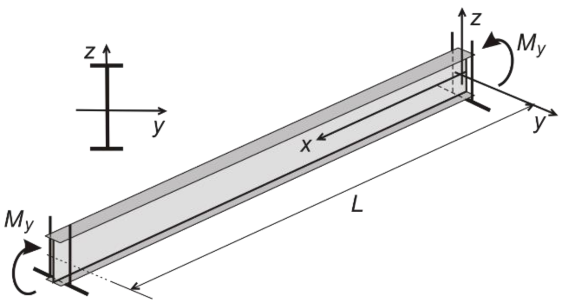

Figure 1: Basic case of lateral-torsional buckling.

In our studies for this basic case, the cross-sections are I-shaped: flange width is 200 mm, the flange and web thickness is 14 and 8 mm, respectively, while total section depth (out-to-out) is 'h', which is variable. In case of these doubly symmetrical I-sections h takes the following values: 150 mm, 180 mm, 200 mm, 300 mm, and 450 mm.

It is known that for this basic case the analytical solution (which is the exact solution of the underlying differential equation system) is expressed as [2]:

$$M_{cr0} = \frac{\pi}{L}\sqrt{EI_z GI_t \left(1 + \frac{\pi^2 EI_w}{GI_t L^2}\right)} \tag{1}$$

Exact or approximate analytical solutions exist for some other cases, but general cases can easier and better be handled by numerical methods.

2.2 Methods: analytical solutions

For the basic case there are analytical solutions in the literature. In fact, at least 4 formulae are proposed, e.g., in [3-5], though some of these formulae were re-derived by other researchers [6-8]. The proposed formulae – in chronological order – are as follows:

$$M_{cr} = M_{cr0} \Big/ \sqrt{\left(1-\frac{EI_z}{EI_y}\right)\left(1-\frac{GI_t}{EI_y}\right)\left(1-\frac{\frac{\pi^2 EI_w}{L^2}}{EI_y\left(1-\frac{GI_t}{EI_y}\right)}\right)} \tag{2a}$$

$$M_{cr} = M_{cr0} \Big/ \sqrt{\left(1-\frac{I_z}{I_y}\right)\left(1-\frac{GI_t}{EI_y}\left(1+\frac{\pi^2 EI_w}{GI_t L^2}\right)\right)} \tag{2b}$$

$$M_{cr} = M_{cr0} \Big/ \sqrt{\left(1-\frac{I_z}{I_y}\right)\left(1-\frac{GI_t}{2EI_y}\left(1+\frac{\pi^2 EI_w}{GI_t L^2}\right)\right)} \tag{3}$$

$$M_{cr} = M_{cr0} \Big/ \left[\left(1-\frac{I_z}{I_y}\right)\left(1-\frac{GI_t}{2EI_y}\left(1+\frac{\pi^2 EI_w}{GI_t L^2}\right)\right)\right] \tag{4}$$

Eq. (4) clearly overpredicts the M_{cr}, which fact was acknowledged even by the authors [5], therefore, this formula is not further discussed here. As far as Eqs. (2a) and (2b) are concerned, though they look different, in fact, they are identical. Finally, Eqs. (2) and (3) are clearly different, but they lead to nearly identical results for practical I-sections. The reason is that the GI_t/EI_y ratio is fairly small for practical I-sections. By assuming that this ratio is negligibly small, both of Eqs. (2) and (3) can be well approximated by the following simple formula:

$$M_{cr} = M_{cr0} \Big/ \sqrt{\left(1-\frac{I_z}{I_y}\right)} \tag{5}$$

This formula in Eq. (5) will be used here for numerical studies.

2.3 Methods: beam finite element

To properly calculate M_{cr} for LTB, a beam finite element method (FEM) is necessary which considers the warping and Saint-Venant torsion of thin-walled members. In this study the Mastan2 software has been employed, which is a free-to-use educational beam finite element software [9].

As in any commercial FEM software, Linear Buckling Analysis is performed on the initial (undeformed) geometry of the structure. In other words, the prebuckling displacements are not considered. If we still want to consider them, an iterative procedure is necessary, as follows:

1. First, we perform classic LBA, and calculate M_{cr} (which, in this step, will be equal to M_{cr0}).
2. We perform linear static analysis to get the deflected shape (i.e., the prebuckling shape), using the Mc as load from the previous Step.
3. We use the deflected shape from the previous step, and perform LBA on the deflected shape, from which we obtain a new value for M_{cr}.
4. Then we repeat steps 2 and 3 till convergence.

Typically, 3-5 iterative steps yield the M_{cr} with appropriate precision.

2.4 Methods: shell finite element

Today, shell FEM is widely considered as a high fidelity method for the linear or nonlinear analysis of thin-walled members. It is employed in innumerable research studies. In our study we have used the commercial software Ansys [10]. The applied finite element is SHELL181, which is a 4-node element with 6 degrees of freedom per node. The out-of-plane behaviour of the element is based on the Reissner-Mindlin plate theory, hence the out-of-plane shear deformations are directly considered. This is mechanically different from the analytical solution and from the beam FEM applied, where the shear deformations are disregarded.

For the discretization of the model, the (average) element size was set to 20 mm. In most of the studied cases the beam was subjected to a concentrated end moment, which was placed onto the model as a set of equivalent line loads at the beam ends, at the edges of the plate elements. The supports were defined so that they imitate the beam-like supports as much as possible.

When the prebuckling deflection is included, it requires the same iterative procedure as described in the previous Section.

2.5 Results

The results of the calculations are summarized in Tables 1 and 2, for beam length of 4 m and 10 m, respectively. To calculate the $\bar{\lambda}$ relative slenderness, the yield strength is assumed to be 235 MPa. The results are visualized by plotting increments of the M_{cr} values due to the prebuckling effect in terms of the flexural rigidity ratio, as shown in Fig. 3.

Table 1: Doubly-symmetric I-sections, basic LTB case, *L*=4 m.

I_y/I_z	$M_{cr0,beam}$ kNm	$M_{cr0,shell}$ kNm	$\bar{\lambda}$ beam	*L*/(max defl) @ $M_{cr,beam}$	increment Eq (5) %	increment beam FEM %	increment shell FEM %
1.46	320.3	311.8	0.52	20	78.6	78.1	63.1
2.20	341.8	333.0	0.56	37	35.5	35.3	30.9
2.78	357.5	348.1	0.58	49	25.0	24.8	22.0
6.85	447.5	434.0	0.67	111	8.2	8.0	7.3
16.93	603.1	577.9	0.74	214	3.1	3.0	2.6

Table 2: Doubly-symmetric I-sections, basic LTB case, *L*=10 m.

I_y/I_z	$M_{cr0,beam}$ kNm	$M_{cr0,shell}$ kNm	$\bar{\lambda}$ beam	*L*/(max defl) @ $M_{cr,beam}$	increment Eq (5) %	increment beam FEM %	increment shell FEM %
1.46	113.0	111.5	0.87	23	78.6	77.9	109.8
2.20	115.2	113.3	0.96	44	35.5	35.3	36.7
2.78	116.8	115.1	1.02	60	25.0	24.8	24.6
6.85	126.3	123.7	1.26	158	8.2	8.1	8.1
16.93	144.3	140.1	1.51	358	3.1	3.0	3.2

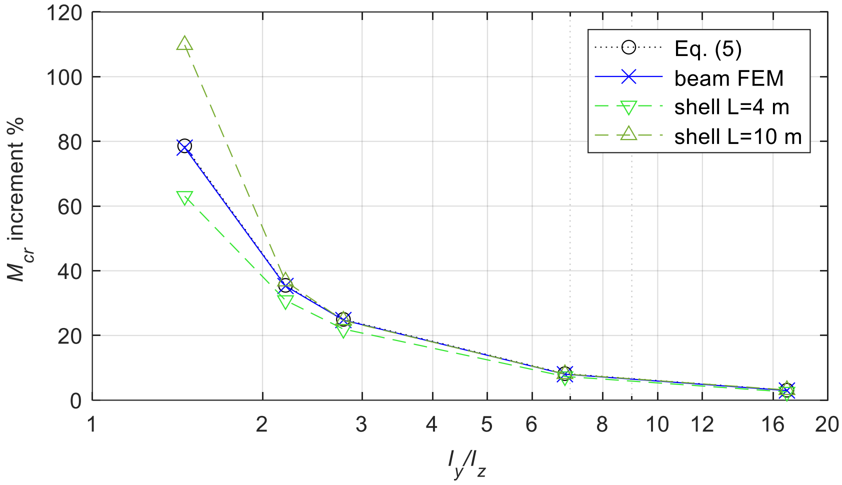

Figure 3: Critical moment increments for the basic case.

It can be observed that the $M_{cr0,shell}$ critical values from the shell FEM are systematically smaller compared to those from beam FEM (which latter ones are identical to those calculated by the classic analytical formula). This observation is not surprising; the shell model is more flexible in the sense that it allows various additional deformations which are out of the realm of classic beam models: out-of-plane shear deformations, transverse plate bending, in-plane shear and in-plane transverse deformations of the plate elements. Though these deformations are small and usually invisible (see Fig. 4), they have some, sometimes non-negligible effect. (Note, this difference can be larger compared to that suggested by Table 1, e.g., by considering other cross-section shapes.)

The effect of prebuckling deformations is clearly observable from the results of any of the methods. Considering the prebuckling deformations increases the critical moment value, but the increase is slightly dependent on which method is used. The increments predicted by Eq. (5) and those predicted by the beam FEM are nearly identical, while increments by the shell FEM are usually slightly smaller. The only exception is when the I_y/I_z ratio is small; in this case the shell FEM predicts significantly different moment increments.

The increment due to the prebuckling deformations is dominantly determined by the flexural rigidities: the smaller the I_y/I_z ratio is, the larger the effect of the prebuckling deformations is. In the case of shell model results the length has some influence, too, which influence is practically non-existent in the beam model. It can be supposed, however, that further factors have importance, too, as discussed in the next Sections.

In Table 1 the deflection values are reported, too, under the effect of the final M_{cr} critical moment, calculated from the beam FEM. (The beam and shell FEM deflections are slightly different, due to, among others, the effect of shear deformations, but the difference is insignificant.) The deflections, in the table, are given as the ratio to the beam length. Not surprisingly, as the depth of the cross-section decreases, the deflection increases, and in the case of the smaller cross-sections the deflection is significant, at least if usual serviceability conditions are assumed. It is to note that this tendency is valid for any other cases presented in this paper, though the actual deflection values are dependent on the actual case (i.e., how the beam is supported, what is the cross-section shape, etc.)

In Table 1, the relative slenderness values are given, too, assuming an ordinary mild steel. As the slenderness values suggest, the reported results cover the range of slendernesses typically found in the practice. This is true for the all the subsequent examples, too.

3 NUMERICAL STUDIES: INFLUENCING FACTORS

3.1 General

In this Section numerical results are presented and briefly discussed, to illustrate how the deviations from the basic LTB case affect the results. Only samples are shown; and as it will be clear from these samples, in most of the cases further analytical and numerical studies are necessary to better understand the phenomena. Since analytical solution hardly exists for anything other than the basic case, we focus on the numerical results. Still, as a reference, the result from the analytical formula of Eq. (5) is given, too.

3.2 End supports

To illustrate the effect of end supports, two cases are considered here: fixed-fixed and pinned-fixed. If the support is "pinned", it corresponds to the basic case, as discussed in the previous Section. If the support is "fixed", it does not mean full fixity, but it means that the rotation around the vertical axis is prevented, as well as the warping is prevented; however, the rotation around the transverse horizontal axis (i.e., *y*-axis) is free to occur.

The calculations have been completed using the doubly-symmetric I-sections as in the previous Section, for beam length of 4 m and 10 m. The results are visualized by plotting the M_{cr} increments due to the prebuckling effect in terms of the flexural rigidity ratio, as shown in Fig. 4.

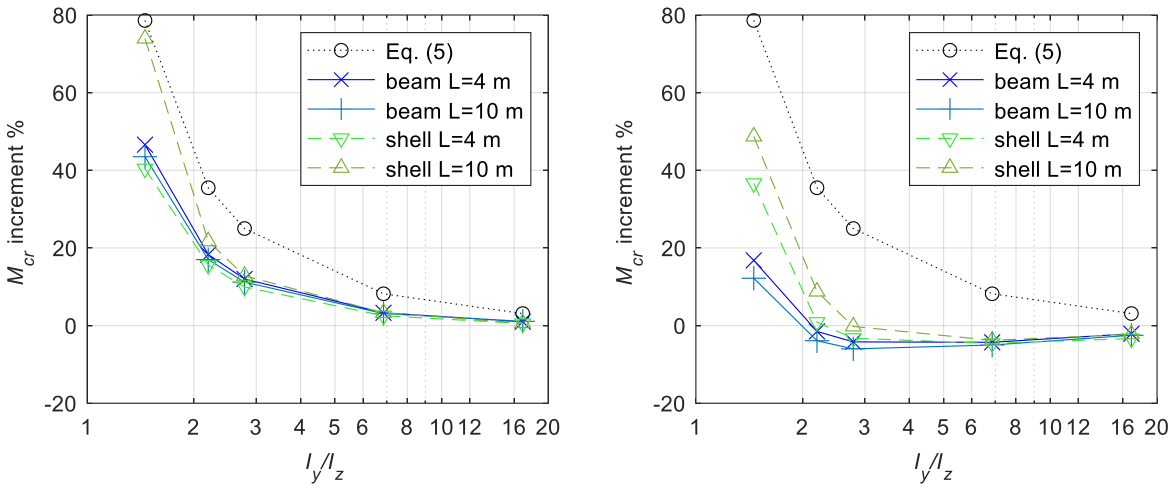

Figure 4: Doubly-symmetric I, uniform moment, left: pinned-fixed, right: fixed-fixed.

The immediate observation is that the effect of the prebuckling deflection is significantly dependent on the end supports. In the presented fixed-fixed case, there is some increment of M_{cr} if the I_y/I_z ratio is small, but for larger (and more practical) I_y/I_z ratios the increment is negative, i.e., the prebuckling deflection decreases the M_{cr}. Even if the reduction is not big, the tendency is just the opposite to what the existing analytical solutions suggest. As far as the pinned-fixed case is concerned, it seems to be in between the fixed-fixed and pinned-pinned cases: the prebuckling deflection increases the critical moment, but the increment is smaller than in the basic LTB case.

The beam FEM and the shell FEM results are similar if the I_y/I_z ratio is not too small. If this ratio is small, there is significant scatter of the predicted critical moment values, depending on the method and also on the beam length, similarly what has been discussed regarding the basic case, in the previous Section.

Moreover, unlike in the pinned-pinned case, even the beam model shows slight dependency of the beam length, i.e., the effect of the prebuckling deflection is slightly decreases as the beam length increases.

3.3 Cross-section shape

To investigate the effect of the cross-section shape, namely the mono-symmetry of the cross-section, three shapes are considered: (a) mono-symmetric I-section, (b) T-section, and (c) C-section. In the case of (a) and (b) the plane of the loading is parallel with the web, i.e., the axis of symmetry is also parallel with the loading plane. In the case of (c) the axis of symmetry is perpendicular to the plane of the loading. The cross-sections are shown in Fig. 5.

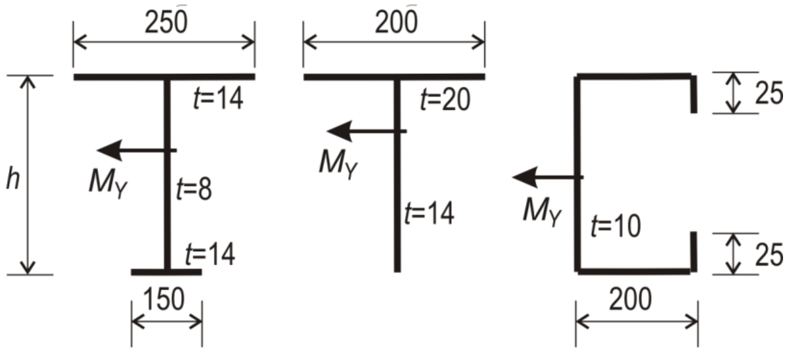

Figure 5: Mono-symmetric cross-sections considered.

It is to note that these cross-sections were selected trying to have realistic geometric proportions and to have global dimensions similar to those of the doubly-symmetric I-sections used earlier. Also, the cross-section depth values were selected so that the I_y/I_z ratios would be similar to those in the previous studies:

(a) h takes the following values, in mm: 170, 200, 220, 330, 500;
(b) h takes the following values, in mm: 190, 220, 240, 330, 460;
(c) h takes the following values, in mm: 200, 250, 280, 440, 680.

The calculations have been completed considering two length values: 4 m and 10 m, in all these cases. The results are shown by plotting the increments of the M_{cr} values due to the prebuckling effect in terms of the flexural rigidity ratio, see Figs. 6-8.

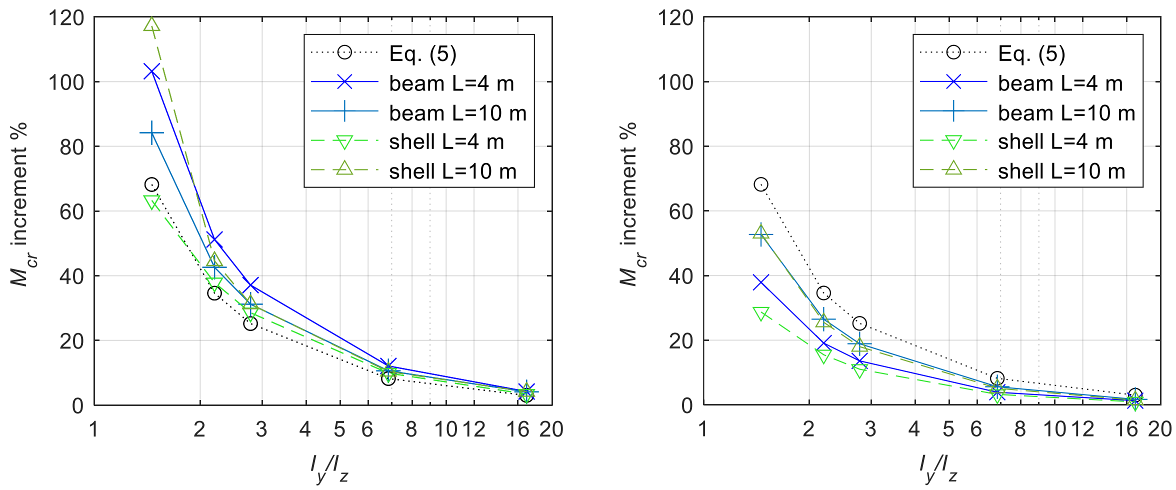

Figure 6: Mono-symmetric I-sections, pinned-pinned, uniform moment,
left: wide flange compressed, right: narrow flange compressed.

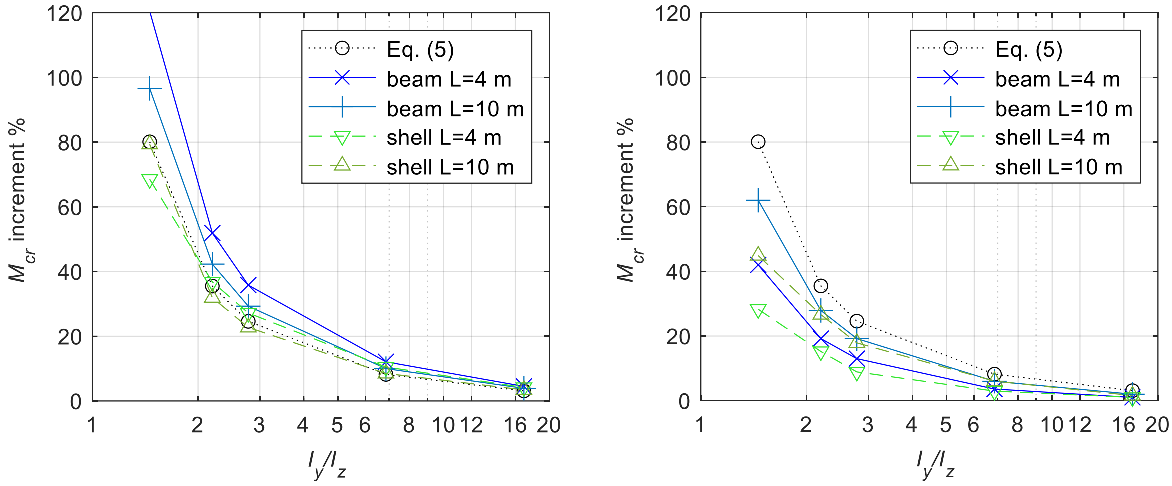

Figure 7: T-sections, pinned-pinned, uniform moment,
left: flange compressed, right: web tip compressed.

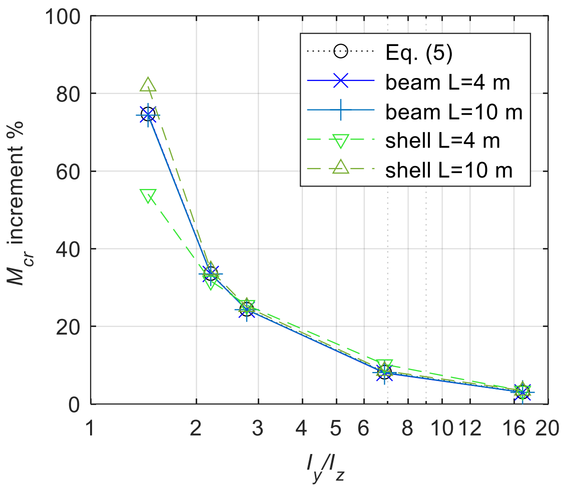

Figure 8: C-sections, pinned-pinned, uniform moment.

It can be observed that cases (a) and (b) are very different from case (c). In the case of the C-section, the observations are identical to those mentioned for the basic case: the beam FEM results and the analytical results are practically identical and length-independent, while the shell FEM results are similar with the exception of small I_y/I_z ratios. At the same time, in the case of (a) and (b) the analytical prediction of Eq. (5) does not work: depending on whether the wider or the narrower flange is compressed, Eq. (5) can under- or overestimate the M_{cr} increment due to the prebuckling deflection. It is interesting to observe that if the narrow flange is in compression, Eq. (5) overpredicts the moment increment, while if the wide flange is compressed, the tendency is unclear, since the various FEM results are significantly different.

3.4 Loading

Two samples are presented here. In both cases the beam is simply supported at both ends, and the cross-section is doubly symmetric I-shaped. In the first one the moment is linearly varying along the length, so that the ratio of the end moments is equal to -0.5. In the second example there are no end moments, but a transverse concentrated force is applied at the middle of the beam. This transverse force acts at the centroid of the cross-sections (which is now identical to the shear center, too). The results are shown by the plots in Fig. 9.

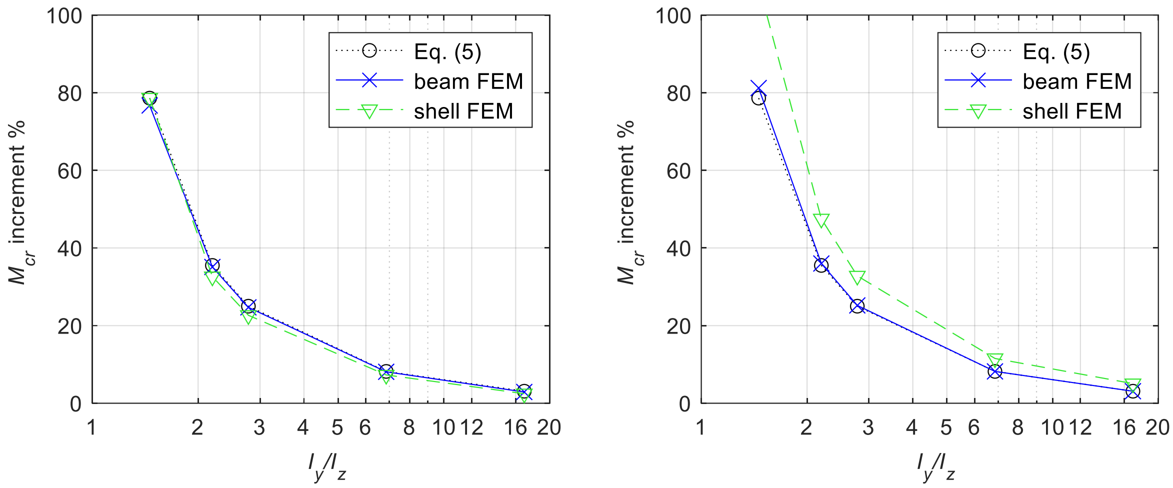

Figure 9: Doubly-symmetric I-sections, pinned-pinned,
left: linear moment, L=10 m, right: concentrated force, L=4 m.

As the plots show, in the case of moment gradient, all the results are close to each other. In the case of the concentrated force loading, the beam FEM and analytical results are still coincident, but in this case the shell FEM increments are somewhat larger. In general, these samples suggest that the loading type has small(er) influence on how the prebuckling deflection modifies the critical moment, but surely, further studies are necessary to better understand the tendencies.

4 CONCLUSIONS

In this paper numerical studies were presented to investigate how the prebuckling deflection of beams influence the critical moment of beams subjected to lateral-torsional buckling. The main conclusions are as follows.

The results prove that the prebuckling deflections modify the results of the linear buckling analysis.

Unlike suggested by the previous literature, the effect of prebuckling deflection is not always positive; it might decrease the critical moment.

The previously proposed analytical formulae to consider the prebuckling effect can be justified for (and only for) certain simple cases, and only if the assumptions of beam models are accepted.

Shell model solutions show tendencies similar to beam models, but the actual numerical values are – sometimes considerably – different.

Our results clearly show that the effect of prebuckling deflection is greatly influenced by the supports and the cross-section asymmetry. On the other hand, the loading type seems to have smaller influence, at least based on a limited number of relevant calculations.

The results presented in the paper prove that the effect of prebuckling deflection on the critical moment of lateral torsional buckling of beams is not fully understood. Further analytical and numerical studies are being performed, the results of which will be reported in the near future.

ACKNOWLEDGEMENT

The presented work was conducted with the financial support of the K138615 project of the National Research, Development and Innovation Office of Hungary.

REFERENCES

[1] Michell, A.G.M., “Elastic stability of long beams under transverse forces”, The London, Edinburgh, and Dublin Philosoph. Mag. J. Sci. 48 (5th ser.): 298, 1899.
[2] Timoshenko, S.P., Z. Math. Phys. 58, 337. 1910.
[3] Trahair, N.S., Woolcock, S.T., “Effect of major axis curvature on I-beam stability”, J. Eng. Mech. Div., ASCE W(EM1): 85-98, 1973.
[4] Vacharajittiphan, P., Woolcock, S.T., Trahair, N.S., “Effect of in-plane deformation on lateral buckling” *Journal of Structural Mechanics*, *3*(1), 29-60, 1974.
[5] Pi, Y.L., Trahair, N.S. “Prebuckling Deflections and Lateral Buckling. II: Applications”, *J. Struct. Eng.* Vol. 118. pp. 2967-2985, 1992.
[6] Roberts, T.M., Azizia, Z.G., “Influence of pre-buckling displacements on the elastic critical loads of thin-walled bars of open cross section”, *Int. J. Mech. Sci.*, Vol. 25, No. 2. pp. 93-104, 1983.
[7] Attard, M.M., Kim, M-Y., “Lateral buckling of beams with shear deformations – A hyperelastic formulation”, *Int Journal of Solids and Structures*, Vol 47, pp. 2825-2840, 2010.
[8] Erkmen, R.E., Attard, M.M., “Lateral–torsional buckling analysis of thin-walled beams including shear and pre-buckling deformation effects”, *Int Journal of Mechanical Sciences*, Vol 53, pp. 918-925, 2011.
[9] Ziemian, R. D., McGuire, W., Liu, S.W., MASTAN2, V5.1.26, 2022.
[10] Ansys, Ansys Inc., Release 2020 R1, 2020.